

Optical studies of gap, hopping energies, and the Anderson-Hubbard parameter in the zigzag-chain compound SrCuO₂

Z. V. Popović,^{1,2,*} V. A. Ivanov,^{1,†} M. J. Konstantinović,³ A. Cantarero,² J. Martínez-Pastor,² D. Olgún,³ M. I. Alonso,⁴ M. Garriga,⁴ O. P. Khuong,¹ A. Vietkin,⁵ and V. V. Moshchalkov¹

¹Laboratorium voor Vaste-Stoffysica en Magnetisme, Katholieke Universiteit Leuven, Celestijnenlaan 200D, B-3001 Leuven, Belgium

²Materials Science Institute, University of Valencia, E46980 Paterna (Valencia), Spain

³Max-Planck-Institut für Festkörperforschung, Heisenbergstrasse 1, D-70569 Stuttgart, Federal Republic of Germany

⁴Institut de Ciència de Materials de Barcelona, Campus de la Universitat Autònoma de Barcelona, 08193 Bellaterra, Spain

⁵Department of Physics, Moscow State University, 119899 Moscow, Russia

(Received 11 April 2000; revised manuscript received 13 September 2000; published 3 April 2001)

We have investigated the electronic structure of the zig-zag ladder (chain) compound SrCuO₂ combining polarized optical absorption, reflection, photoreflectance, and pseudo-dielectric-function measurements with the model calculations. These measurements yield an energy gap of 1.42 eV (1.77 eV) at 300 K along (perpendicular to) the Cu-O chains. We have found that the lowest-energy gap, the correlation gap, is temperature independent. The electronic structure of this oxide is calculated using both the local-spin-density approximation with gradient correction method and the tight-binding theory for the correlated electrons. The calculated density of electronic states for noncorrelated and correlated electrons shows quasi-one-dimensional character. The correlation gap values of 1.42 eV (indirect transition) and 1.88 eV (direct transition) have been calculated with the electron hopping parameters $t=0.30$ eV (along a chain), $t_{yz}=0.12$ eV (between chains), and the Anderson-Hubbard repulsion on copper sites $U=2.0$ eV. We concluded that SrCuO₂ belongs to the correlated-gap insulators.

DOI: 10.1103/PhysRevB.63.165105

PACS number(s): 78.40.-q, 71.27.+a, 71.15.Ap, 71.20.Ps

I. INTRODUCTION

Strontium copper oxide, SrCuO₂, belongs to the new family of quasi-one-dimensional (1D) insulators whose properties have been a subject of intensive studies in recent years.¹⁻¹² This oxide, grown in single-crystalline form under ambient pressure, has an orthorhombic unit cell (space group D_{2h}^{17} , $Cmcm$) with parameters $a=3.577$ Å, $b=16.342$ Å, $c=3.9182$ Å, $Z=4$.^{13,14} SrCuO₂ has a unique structure consisting of CuO₄ squares, mutually connected via common edges, that form double copper zigzag chains (Fig. 1).

Magnetic susceptibility measurements of SrCuO₂ have revealed that the Cu²⁺ moments order antiferromagnetically below ~ 2 K.⁴ The exchange interaction energy J is estimated to be 2100 ± 200 K.⁵ Very recently, a static disorder spin structure (spin freezing) rather than static three-dimensional long-range spin order is found in SrCuO₂ using neutron spectroscopy.¹⁵ An angle-resolved photoemission spectroscopy (ARPES) study of SrCuO₂ shows the spin-charge separation in this oxide, as a consequence of electron correlations.^{2,3} The optical phonons in SrCuO₂ have been investigated by measuring Raman scattering⁶⁻⁹ and far-infrared reflectivity spectra on polycrystalline⁷ and single-crystal⁹ samples.

The electronic structure of SrCuO₂ has been calculated using the linear-augmented-plane-wave (LAPW) method within the local-density approximation (LDA) to the density-functional theory.¹⁰ As noted in Ref. 10 for this type of calculations the agreement with the ARPES data takes place only in the region far from the Fermi level. Most recent band-structure calculations^{11,12} by the local-spin-density approximation (LSDA), including an on-site Coulomb repul-

sion (LSDA+ U method) have produced an insulating gap of 1.63 eV for $U=12.3$ eV (Ref. 11) and 2.36 eV for $U=5$ eV (Ref. 12). Due to the lack of experimental data for the energy gap of SrCuO₂, it was not possible to compare these data with experiments. Quite recently, Rosner *et al.*¹⁶ calculated the electronic structure of SrCuO₂ using the LSDA method, also. They found that the gap in the antifer-

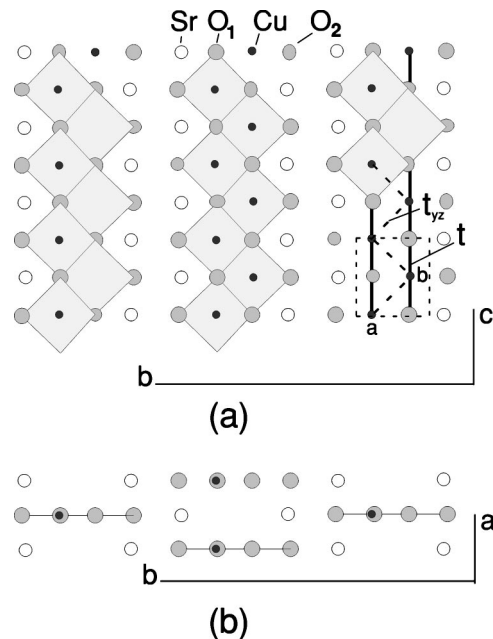


FIG. 1. Crystal structure of SrCuO₂ in the (a) (100) and (b) (001) plane. Dashed line rectangle represents a unit cell of the zigzag ladder.

romagnetic phase of SrCuO₂, reported in previous publications,^{11,12} is probably artificial and appears due to too small number of the \mathbf{k} points in the Brillouin zone taken in the computation procedure.

In this paper we have applied complementary optical spectroscopy techniques to study the electronic structure of SrCuO₂. We have obtained an energy gap of 1.42 eV (1.77 eV) at 300 K along (perpendicular to) the Cu-O chains. These values are compared with the results of the electronic structure calculations completed by us. We have established that the tight-binding method for the correlated electrons, with the hopping parameters $t=0.30$ eV and $t_{yz}=0.12$ eV along legs and between legs, respectively (see Fig. 1) and the Anderson-Hubbard parameter $U=2.0$ eV yields the energy gap values in agreement with the experimental results. We also have determined the density of electronic states for non-correlated and correlated electrons, which show the one-dimensional nature. According to the electronic structure calculations and the experimental findings, we concluded that SrCuO₂ is a correlated-gap insulator.

The remainder of this paper is organized as follows. Experimental details are given in Sec. II. The results of electronic structure calculations for noncorrelated electrons (using the LSDA with gradient corrections to density-functional theory) are described in Sec. III A. The reason why we use this method is to obtain the data necessary for the determination of the correlated electronic structure and to compare our results with the previously published ones.^{10–12,16} In Sec. III B, we applied the tight-binding theory for correlated electrons taking into account the realistic crystalline structure of SrCuO₂. We obtained analytically the energy dispersion relations and the density of states of correlated and noncorrelated electrons as well as the correlation gap. Experimental measurements of dielectric function, reflectivity, photoreflectance, and optical transmission spectra are given in Sec. IV. Section V contains the discussion of experimental and theoretical results and the conclusions.

II. EXPERIMENTAL DETAILS

The present work was performed on a single-crystal sample with a size of about 15, 2, and 6 mm along the \mathbf{a} , \mathbf{b} , and \mathbf{c} axes, respectively. We used several optical spectroscopy techniques. The pseudo-dielectric-function was measured with the help of a rotating-polarizer (analyzer) ellipsometer. A Xe lamp was used as a light source, a double monochromator with 1200-lines/mm gratings, and an S20 photomultiplier tube as a detector. The polarizer and analyzer were Rochon prisms. The measurements were carried out in the 1.2–5.6-eV energy range. For the energies below 1.6 eV we used a halogen lamp as a light source and Si photodiode as a detector. Optical reflectivity and transmission spectra were measured at room and liquid-helium temperature in the 200–2500-nm spectral range with Perkin-Elmer Lambda 19 spectrophotometer. Photoreflectance measurements were performed at room temperature under incident polarized light parallel to the \mathbf{a} and the \mathbf{c} axes. The reflected light was dispersed through a single $\frac{1}{2}$ -m monochromator and synchronously detected by a Si photodiode.

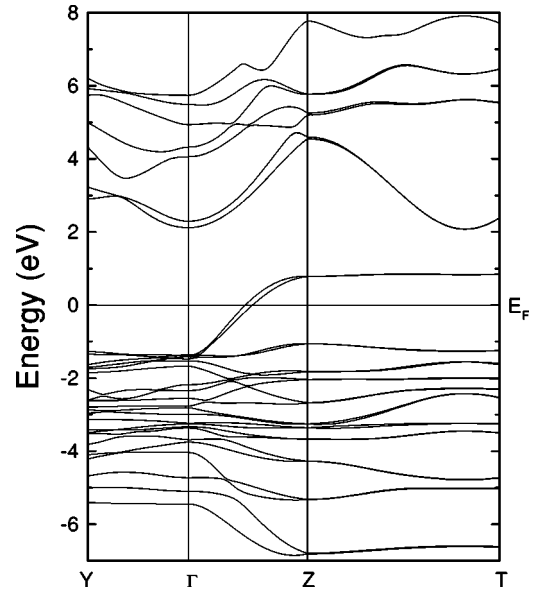


FIG. 2. Electronic structure of SrCuO₂ along the several high-symmetry directions in the BZ calculated using the LSDA with the gradient correction method. The Cartesian coordinates of high-symmetry points are as follows: Γ (0,0,0); Y ($2\pi/a,0,0$), ($0,2\pi/b,0$); Z ($0,0,\pi/c$); T ($2\pi/a,0,\pi/c$), ($0,2\pi/b,\pi/c$).

III. ELECTRONIC STRUCTURE CALCULATIONS

A. LSDA with gradient corrections

In the CuO₂-layered oxides, the electron dispersion branches at the Fermi level are derived from the $3d_{x^2-y^2}$ copper orbitals, mixed with the corresponding O $2p$ orbitals. Other occupied $3d$ Cu orbitals ($d_{3z^2-r^2}, d_{yz}, d_{xz}, d_{xy}$) are located below the Fermi level and they are strongly hybridized with oxygen bands. These cuprates are known as charge-transfer insulating oxides. In contrast to the CuO₂-layer cuprates (tetragonal crystal structure oxides), SrCuO₂ has an orthorhombic crystal structure with the Cu-O zigzag chains and, consequently, with the different electronic structure, as it will be shown later.

For the *ab initio* calculation of the electronic structure of SrCuO₂ we used WIEN97 software package.¹⁷ The program allows us to compute the electronic structure within the density-functional theory by applying the LAPW method with a simplified version of the generalized gradient approximation¹⁸ for the exchange-correlation functional in the LSDA description. This approximation takes into account the charge and spin inhomogeneity in a material by including gradient corrections in the energy functional and gives more precise ground-state energy¹⁹ but does not improve the quasiparticle spectra.²⁰

Figure 2 shows the calculated electron energy dispersions along the high-symmetry lines of the Brillouin zone (BZ). The most interesting feature of these calculations is a relatively large dispersion along the k_z direction parallel to the Cu-O chains and dispersionless bands perpendicular to them, i.e., along the k_x and k_y directions. Along the Γ -Z direction of the BZ, the two bands, which cross the Fermi level, split slightly, indicating that the interaction between the two neighboring chains in the ladder is small but still exists. The

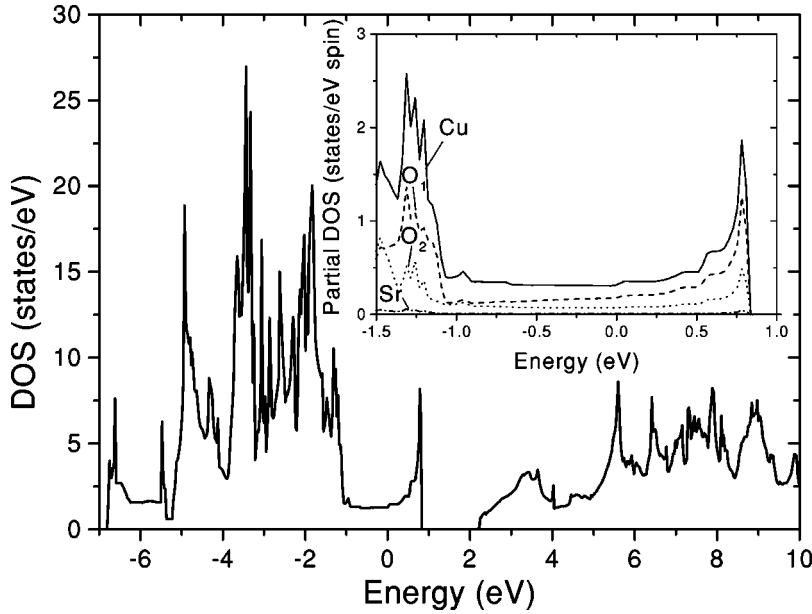


FIG. 3. Total density of states calculated within the LSDA with the gradient correction method. Inset: Partial density of states close to Fermi level of different atoms of SrCuO₂.

total density of electronic states of SrCuO₂ is given in Fig. 3 in the energy range between -7 and 10 eV. The electron density of states is calculated with 180 \mathbf{k} points in the irreducible part of the BZ and it is in an agreement with previous publications.^{10,16} Because the main properties depend on the electrons at the Fermi level, we paid special attention to the energy dispersions near E_F . In the inset of Fig. 3 we show the partial density of electronic states in the energy range from -1.5 to 1 eV. Figure 4 gives the contribution from the different Cu $3d$ and O $2p$ orbitals to the partial density of states in the energy range close to the Fermi level. From the results given in Figs. 2–4 we concluded the following.

(i) The electronic structure of SrCuO₂ is a quasi-one-dimensional one.

(ii) The main contribution to the density of states in SrCuO₂ near the Fermi level comes from the Cu $3d_{y^2-z^2}$ orbitals.

(iii) There is a small hybridization between the Cu $3d_{y^2-z^2}$ and the O $2p_z$, $2p_y$ orbitals.

These results are in an agreement with the x-ray absorption spectroscopy data,²¹ which show that the holes in SrCuO₂ have predominantly $3d_{y^2-z^2}$ character (which is analogous to the Cu $3d_{x^2-y^2}$ orbitals in notation for the 2D high- T_c cuprates). The hole occupancy of $3d_{3x^2-r^2}$ is less than 5%.²¹ However, the metallic state obtained in the framework of the LSDA calculation (in Figs. 2–4 the Fermi level $E_F=0$ is inside the occupied band) does not allow us to compare these results with our experiments.

The applied LAPW method with the gradient LSDA corrections (or other LDA versions to the density functional) employs the orbitally independent exchange-correlation potential, which cannot recognize different d orbitals in the copper ion with an open d atomic shell, Cu¹⁺ⁿ($3d^{10-n}$), of the SrCuO₂ material. As a result it gives a satisfactory band structure, but cannot overcome “an energy-gap problem.”²² In general, the local approximations to the density-functional theory (for a review see Ref. 22 and Refs. 23–25 for an

inclusion of the spin-dependent exchange-correlation potentials) are successful in describing the ground-state energies and the quantities, weakly depending on a charge or spin density,^{26,27} but the excited states are beyond the scale of the density-functional theory.

To alleviate an energy-gap problem of L(S)DA to density-functional theory the LDA+ U method has been proposed

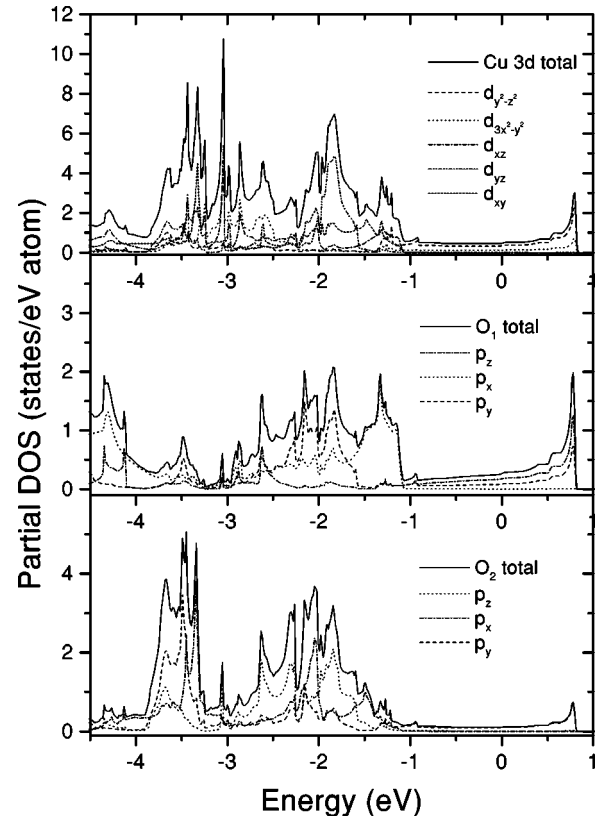


FIG. 4. The contribution of different orbitals to the calculated partial density of states (DOS) of SrCuO₂. (a) Cu- d DOS, (b) O1- p DOS, and (c) O2- p DOS.

[for details see Ref. 28 and its generalization, LSDA+ U (Ref. 29)]. These methods have extended LDA-like functionals with an addition to them the on-site Hubbard terms and they are based on the unrestricted Hartree-Fock wave functions. For the Mott-Hubbard insulating compounds with transition or rare-earth metals the orbital-dependent potential U leads to splitting of the partially filled $3d$ or $4f$ bands forming the upper and the lower Hubbard-like bands. The LDA+ U functional gives more correct antiferromagnetic properties than the LSDA functional. Also LDA+ U functionals are relevant for study of the temperature-induced phase transition from a nonmagnetic insulator to a metal with a local magnetic moments and for study of the charge orders, where LSDA fails. However, the mean-field correction used for a single orbital, $U\hat{n}_\uparrow\hat{n}_\downarrow \rightarrow U\hat{n}_\uparrow n_\downarrow$ (n_\downarrow is an expectation value for the number of electrons with a spin projection \downarrow occupying a fixed partially filled orbital on a particular lattice site), for an exchange-correlation potential reproduces only qualitatively the correct physics for the Mott-Hubbard insulators. Inclusion of the interorbital intra-atomic interactions (Coulomb repulsion and Hund exchange) and often the antiferromagnetic ordering³⁰ (regardless the absence of an antiferromagnetism in material under consideration; e.g., SrCuO₂ is in paramagnetic state above 1.4 K) does not change significantly the qualitative character of the LDA+ U results. The obtained gap values differ by about 1 eV from the experimental ones.^{28,29} Also in the framework of LDA+ U methods the band structure is unsatisfactory, and these methods produce unphysical insulating states for transition metals since the LDA+ U functionals split even the partially filled bands due to the self-interaction corrections both for localized and extended electron states. It is also known that the electron correlations produce narrowing of the dispersion branches and consequently an increase of the effective masses,^{31–33} which is outside the LDA+ U domain.

As applied to SrCuO₂, the band-gap values obtained in the LDA+ U calculations^{11,12} differ significantly from our experimental findings (see Sec. IV). Besides that, a shift of the energy bands due to a finite U cannot guarantee the correct band extrema positions to identify the direct or indirect character of the interband electronic transitions. In Ref. 11 the reported band gap 1.63 eV (the closest to our measured value) corresponds to an unrealistically large Anderson-Hubbard parameter $U=12.3$ eV. Having all above in mind, we developed a model that *introduces the electron correlations already in the zeroth order of the applied perturbation theory* with respect to the hopping energies in a realistic lattice structure of SrCuO₂ (Sec. III B).

B. The tight-binding method for the correlated electrons

According to our LSDA data (Figs. 2–4) and also Ref. 21, the main contribution to the electron density of states close to the Fermi level comes from the $d_{y^2-z^2}$ orbitals, slightly hybridized with the O $2p$ orbitals. In addition, our absorption measurements (see Sec. IV) show that the lowest-energy gap is practically temperature independent (a charge-transfer gap depends on temperature in accordance with the variation of the Cu-O distance with temperature). All these important ob-

servations have lead us to the conclusion that the band gap in SrCuO₂ is a consequence of strong electron correlations, favoring the Mott-Hubbard-like insulating state.

Although the density-functional theory reduces the Schrödinger equation for electrons and atomic nuclei in solids to nonlinear single-particle equations (equations with self-consistent potential, which itself depends on the solutions of the equations), the explicit dependence of the ground-state energy on the ground-state charge and spin density is unknown, and such an explicit functional may even not exist. As the starting many-body linear Schrödinger equation, the problem of the nonlinear single-particle equations with the exchange-correlation potentials is a formidable problem that cannot be solved without additional approximations. The exchange and correlations are often approximated by the L(S)DA according to which the charge (spin) density in the exchange-correlation potential of an electron gas or a jellium model is replaced by the local density in a real material. The strategy of the LDA approach is close to the Landau Fermi-liquid theory, where the energy is a functional with respect to a single-particle partition function. But contrary to the Landau theory, the density-functional theory can calculate only the ground-state energy, distributions of charge and spin densities, and the quantities connected with them. The main problem in our case is that LDA and its versions (e.g., the one used by us) do not give a clear knowledge about the Anderson-Hubbard parameter (an essential on-site repulsion of the correlated electrons) in narrow-energy-band materials such as SrCuO₂.

The conventional tight-binding method ($U=0$) for an electronic structure in solids is self-contradictory. According to it the eigenfunctions of the Schrödinger equation are approximated using the electron wave functions of the isolated atoms, i.e., a conventional tight-binding method is more suitable the greater interatomic distances in the crystal. But in this case the prevailing terms in the Hamiltonian, the strong electron-electron interactions U , become even larger; they cannot be reduced to any mean-field version, and then the problem is fully outside the domain of the standard Slater-Koster scheme. The present tight-binding method for correlated electrons is based on the hypothesis that the narrow-energy band material properties, e.g., SrCuO₂ in our case, are governed by the intra-atomic electron correlations U , exceeding considerably the transfer energies.

A reasonable simulation of the many-body effects leads to tremendous problems in terms of the conventional Fermi- or Bose-operator permutation relations that do not encompass all possibilities of the second quantization formalism. The permutation relations for the Okubo-Hubbard X operators are linear with respect to themselves operators. The necessity to introduce the operators with more complicated permutation relations than the fermionic and bosonic relations for study of the electron correlations was indicated by Bogoljubov already in 1949.³⁴ We consider the tunneling part of any correlated Hamiltonian as a perturbation with respect to the strong electron correlations included in the unperturbed part of the Hamiltonian. The Hamiltonians with correlated electrons are rewritten in terms of the basis and only basis vectors of the corresponding superalgebra. To treatment of such

Hamiltonians in the X -operator framework is based on a rigorous successive method that we followed in our previous publications^{35–37} and it will be also applied here. The systematic perturbation theory is based on the generalized Wick theorem as an iteration procedure reducing the time-ordered product of n X operators to a product of $n-1$ X operators. The first-order self-energy is the tunneling matrix itself from the perturbative Hamiltonian.

Here in the framework of the $su(2,2)$ superalgebra approach for the $SrCuO_2$ system we will neglect the scattering of the correlated copper electrons by the spin and charge fluctuations, aiming at comparing the electron spectra with the conventional tight-binding calculations, which are done to first order of the transfer energy. Contrary to the standard Hubbard model for the s electrons with a single site per a unit cell, the starting Hamiltonian includes a realistic unit cell (a few sites) and the correlated electrons with the non-zero angular momenta. In the framework of the *presented tight-binding method for the correlated electrons* the non-spherical wave functions provide anisotropy of the hopping integrals in the lattice. In the considered order of the perturbation theory we will concentrate on the influence of the band-structure effects, which are of significance for multi-component systems such as $SrCuO_2$.

The LSDA calculation of the electronic structure of $SrCuO_2$, Figs. 2–4, revealed that electron energy dispersions are governed mainly by electrons in the zigzag ladder. The interladder coupling is negligible because of the large (6.75-Å) Cu atom distance between neighboring ladders. A unit cell for the correlated electron structure calculation includes two Cu ions only, as indicated by a dashed-line rectangle in Fig. 1(a). We assume that a ladder unit $Cu^{1+n}O_2^{2-}$ has a total charge -2 , i.e., there is one hole, $n=1$, per a copper ion in the ladder. In our minimal model, we neglected hybridization with the p_y, p_z orbitals of the intermediate oxygen atoms, assuming the $d_{y^2-z^2}$ character of holes. Such

an approximation is common for the 1D cuprates³⁸ because the Anderson-Hubbard repulsion usually opens a gap between the $3d$ bands. Inside the ladder, the arrangement of the Cu atoms is such that the directions from the Cu ion in one leg to the two nearest Cu ions of the neighboring leg are almost at a right angle ($\sim 90^\circ$); see Fig. 1. In our consideration of the electronic structure we assume that these directions form an ideal right angle and the electron energy dispersions are governed mainly by the correlated electrons in the single zigzag ladder.

Aiming at the determination of the Anderson-Hubbard parameter U from the optically measured correlation-gap values, the further theoretical study is based on the realistic Hamiltonian with one copper rung/dimer, $a-b$, per unit cell:

$$H = -2t \sum_{p,\sigma} \cos p_z [a_\sigma^\dagger(p) a_\sigma(p) + b_\sigma^\dagger(p) b_\sigma(p)] - t_{yz} \times \sum_{p,\sigma} (1 + e^{-ip_z}) [a_\sigma^\dagger(p) b_\sigma(p) + \text{H.c.}] + U \times \sum_{i=a,b} n_{\uparrow i}^j n_{\downarrow i}^j - \mu \sum_{i=a,b} n_i^j, \quad (1)$$

where a, b denote chains (legs in the ladder directed along the c axis), t is an amplitude of the carrier hopping along the legs, t_{yz} is a diagonal hopping amplitude between the legs, U is the Anderson-Hubbard repulsion of the $d_{y^2-z^2}$ electrons on the copper site, and μ is the chemical potential. In LDA band-structure calculations the electron-electron interactions are approximated by an effective single-electron problem, whereas in our approach the Anderson-Hubbard parameter U is included explicitly in the nonperturbative Green's function. Applying the X -operator procedure,³⁷ the correlated energy bands are governed by zeros of the inverse Green's function for the first-order X operators with respect to the tunneling matrix:

$$\hat{D}_p^{-1}(\omega) = \begin{array}{l} a \\ b \end{array} \begin{array}{l} \left\{ \begin{array}{l} 0+ \\ -2 \end{array} \right. \\ \left\{ \begin{array}{l} 0+ \\ -2 \end{array} \right. \end{array} \left(\begin{array}{cccc} \frac{-i\omega_n - \mu}{f_{0+}} + r & r & v & v \\ r & \frac{-i\omega_n - \mu + U}{f_{-2}} + r & v & v \\ v^* & v^* & \frac{-i\omega_n - \mu}{f_{0+}} + r & r \\ v^* & v^* & r & \frac{-i\omega_n - \mu + U}{f_{-2}} + r \end{array} \right), \quad (2)$$

where $r = -2t \cos p_z$ and $v = -t_{yz}(1 + e^{-ip_z})$. Here the correlation factors, $f_{0+(-2)}$, in the diagonal Green's functions are determined by the fermion occupation n per site. For a considered nonmagnetic phase of $SrCuO_2$ they are $f_{0+} = 1 - n/2$, $f_{-2} = n/2$ and are all equal to $\frac{1}{2}$ ($n=1$). After an analytical continuation, $i\omega_n \rightarrow \xi + i\delta$, from the secular equation

$|\hat{D}_p^{-1}(\omega)| = 0$ one can find the four branches of the correlation energy dispersions in an explicit form:

$$\xi_B^\pm(p) = \varepsilon_p^{1,2} + \sqrt{(\varepsilon_p^{1,2})^2 + \left(\frac{U}{2}\right)^2} - \mu, \quad (3)$$

$$\xi_A^\pm(p) = \varepsilon_p^{1,2} - \sqrt{(\varepsilon_p^{1,2})^2 + \left(\frac{U}{2}\right)^2} - \mu, \quad (4)$$

where $\varepsilon_p^{1,2} = -t \cos p_z \pm t_{yz} \cos(p_z/2)$. For the derivation of these energy dispersions from the 4×4 secular equation [see Eq. (2)] it was useful to apply the proved theorem about the decomposition of the determinant with respect to diagonal elements (see Appendix A in Ref. 39).

The lower correlated subbands, ξ_A^+ , and ξ_A^- , are completely occupied by the two holes from a unit cell of the zigzag ladder. It is essential that the chemical potential μ should be found self-consistently from the equation for a particle density,

$$n = T \sum_{p, \omega, \alpha, \beta} e^{i\omega\delta} D_{\alpha, \beta}(p, \omega_n),$$

where α and β label the rows and columns of the Green's-function elements [cf. Eq. (2)]. For $n=1$ (the case of SrCuO₂) the calculated chemical potential is positioned in the middle of the energy gap ($\mu=0$). For other densities, $n \neq 1$, the procedure used generates a correlated metal. The upper correlated subbands, ξ_B^\pm , are empty for SrCuO₂. The nearest unoccupied energy band is ξ_B^- and the correlation gap (indirect transition; see Fig. 5) in an electronic structure can be estimated as

$$\begin{aligned} \Delta_0 &= \min \xi_B^-(p) - \max \xi_A^+(p) \\ &= \sqrt{(t+t_{yz})^2 + \left(\frac{U}{2}\right)^2} + \sqrt{\left(t + \frac{t_{yz}^2}{8t}\right)^2 + \left(\frac{U}{2}\right)^2} \\ &\quad - \left(2t + t_{yz} + \frac{t_{yz}^2}{8t}\right). \end{aligned} \quad (5)$$

For the noncorrelated energies, $\varepsilon^{1,2} = 2\varepsilon_p^{1,2}$ [cf. Eqs. (3) and (4)], the electron density of states per atom, $\rho_0(\varepsilon) = \sum p_z [\delta(\varepsilon - \varepsilon^{(1)}) + \delta(\varepsilon - \varepsilon^{(2)})]$, is defined analytically as follows:

$$\rho_0(\varepsilon) = \frac{1}{\pi \sqrt{t_{yz}^2 - 4t(\varepsilon - 2t)}} \sum_{i=1}^4 \frac{1}{\sqrt{1 - x_i^2}}, \quad (6)$$

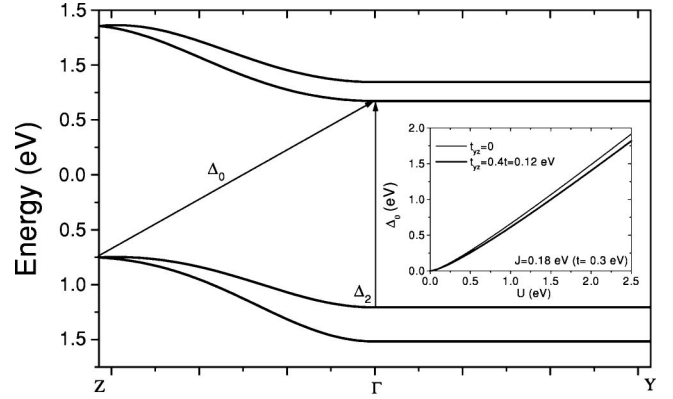
where

$$x_{1,2} = \frac{1}{4t} [-t_{yz} \pm \sqrt{t_{yz}^2 - 4t(\varepsilon - 2t)}] = -x_{4,3}. \quad (7)$$

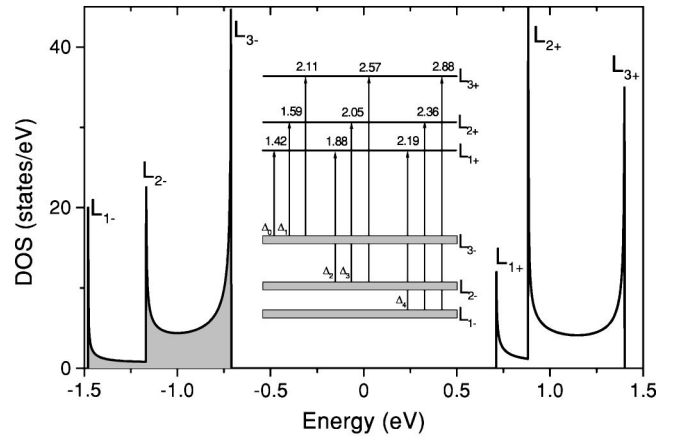
The electron-electron repulsion U splits the density of the noncorrelated electron states $\rho_0(\varepsilon)$. After the transformation to the ‘‘correlated’’ variables, Eqs. (3) and (4), one can get the correlated electron density of states as

$$\begin{aligned} \rho(\xi) &= \frac{\xi^2 + (U/2)^2}{\xi^2} \rho_0\left(\frac{\xi^2 - (U/2)^2}{\xi}\right) \\ &= \frac{\xi^2 + (U/2)^2}{\xi^2} \sum_{p, \alpha=A, B} \frac{\xi_\alpha^2(p)}{\xi_\alpha^2(p) + U^2} \delta\left(\xi - \frac{\xi_\alpha(p)}{2}\right). \end{aligned} \quad (8)$$

Figure 5(a) shows the correlated electron energy dispersions [Eqs. (3) and (4)] along the Z and the Y symmetry



(a)



(b)

FIG. 5. (a) The tight-binding dispersions for correlated electrons in SrCuO₂ with parameters $t=0.3$ eV, $t_{yz}=0.12$ eV, $U=2.0$ eV. The momenta are given in units $|p_y\sqrt{2}| = |p_z| = \pi$ of the Brillouin-zone boundaries, the Fermi energy $E_F=0$ is inside of the correlation gap. Inset: energy gap vs U dependence for $t_{yz}=0$ and 0.12 eV. (b) The correlated electron density of states as a function of energy. The electronic structure parameters are the same as for (a). Inset: the energy values of all possible transitions between occupied and empty states.

directions of the BZ. The correlated electron density of states is given in Fig. 5(b). The overlap of the energy ranges for the energy dispersions, Eqs. (3) and (4), leads to the appearance of singularities at

$$\xi_1^{B,A} = \xi_{B,A}^-(p_z=0) - S,$$

$$\xi_2^{B,A} = \xi_{B,A}^+(p_z=0) - S,$$

$$\begin{aligned} \xi_3^{B,A} &= t + (1 - \alpha) \frac{t_{yz}^2}{8t} + (2\alpha - 1)S \\ &\quad + \alpha \left[t_{yz} + \sqrt{(t+t_{yz})^2 + \left(\frac{U}{2}\right)^2} \right], \end{aligned}$$

where

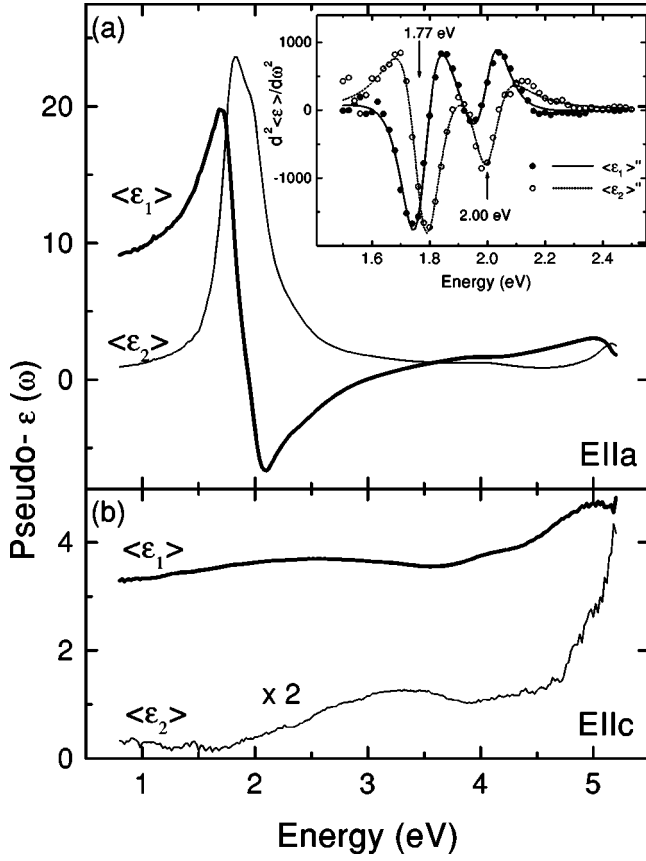


FIG. 6. Room-temperature real (ϵ_1) and imaginary (ϵ_2) part of the pseudo-dielectric-function of SrCuO₂. The spectra of the (010) surface taken with (a) the **a** axis (**E**||**a**) and (b) the **c** axis (**E**||**c**), parallel to the plane of incidence. Inset: second derivative of dielectric functions for **E**||**a** polarization in the 1.5–2.5-eV spectral range.

$$S = \frac{1}{2} \left[\sqrt{(t+t_{yz})^2 + \left(\frac{U}{2}\right)^2} - \sqrt{\left(t + \frac{t_{yz}^2}{8t}\right)^2 + \left(\frac{U}{2}\right)^2} + \frac{t_{yz}^2}{8t} - t_{yz} \right],$$

and α takes sign +1 and -1 for the correlated subbands B [Eq. (3)] and A [Eq. (4)], respectively. The van Hove square-root divergencies inside the correlated bands are manifestations of the quasi-one-dimensional electronic structure. The comparison of the calculated electronic structure with the measured optical transitions allows us to estimate the Anderson-Hubbard parameter and the hopping energies of correlated electrons in the zigzag-ladder compound SrCuO₂.

IV. EXPERIMENTAL RESULTS

Figure 6 shows the pseudo-dielectric-function $\epsilon(\omega) = \epsilon_1(\omega) + i\epsilon_2(\omega)$ for a light polarized parallel to the **a** axis [Fig. 6(a)] and the **c** axis [Fig. 6(b)]. As it can be seen from Fig. 6(a), the maximum of $\epsilon_2(\omega)$ is at about 1.77 eV. This value corresponds to the energy gap along the **a**-axis direction, which is perpendicular to the CuO chains. Besides the most intensive peak at 1.77 eV, we found the next peak at

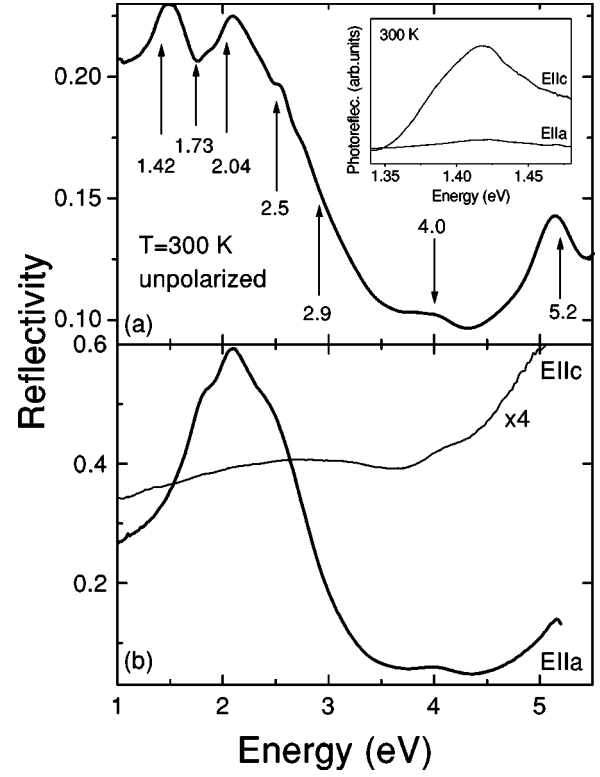


FIG. 7. (a) Room-temperature unpolarized reflectivity spectra of the SrCuO₂ single crystal. (b) Reflectivity spectra calculated using experimental data of the pseudo-dielectric-function from Fig. 6. Inset: polarized photoreflectance spectra at room temperature.

about 2 eV. To determine the precise energies of these electronic transitions we fitted both the real and the imaginary parts of the second derivative spectra $d^2\epsilon/dE^2$ simultaneously by a least-squares routine in terms of standard line shapes:

$$\epsilon(\omega) = C - Ae^{i\phi}(\omega - E_0 + i\Gamma)^m,$$

where A , E_0 , and Γ are the amplitude, energy, and half line-width of the electron transitions, respectively. The ϕ is a phase factor and the exponent m has the value $-1/2$ for the one-dimensional case. The results of the calculations are given in the inset of Fig. 6(a). At higher energies we observed two additional peaks at about 4.1 and 5.1 eV. The origin of all these transitions will be discussed later. For **E**||**c** polarization the first clearly pronounced peak appears at about 3.2 eV, and the next maxima is at about 5.2 eV [see Fig. 6(b)]. For this polarization the low intensity of the dielectric function does not allow us to apply the same fitting procedure as in the **E**||**a** case.

An unpolarized reflectivity spectrum is shown in Fig. 7(a) in the energy range from 1 to 5.5 eV. The peak positions at 1.42, 1.73, 2.04, 2.5, 2.9, 4, and 5.2 eV are determined as the maxima of an optical conductivity function obtained from the Kramers-Kronig analysis of the reflectivity spectrum. In order to distinguish different polarization contributions in the reflectivity spectrum shown in Fig. 7(a), we calculated the polarized reflectivity spectra using the pseudo-dielectric-function data from Fig. 6. The results of the calculations are

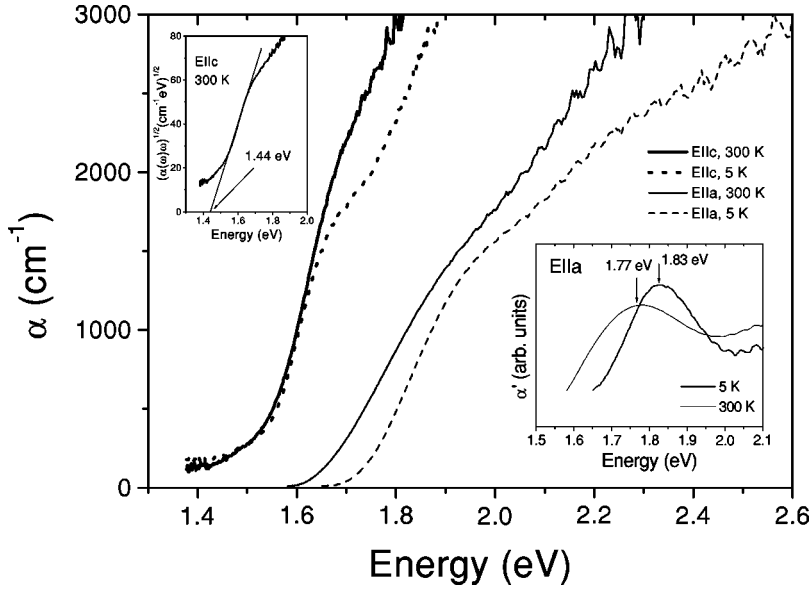


FIG. 8. Absorption coefficient spectra of SrCuO_2 at room and liquid-helium temperatures. Inset, left panel: $\sqrt{\alpha(\omega)}$ vs ω dependence. Inset, right panel: first derivative of $\alpha(\omega)$ dependence for $\mathbf{E}\parallel\mathbf{a}$ polarization.

given in Fig. 7(b). As it can be seen from Fig. 7(b), the main contribution to the unpolarized spectra comes from the $\mathbf{E}\parallel\mathbf{a}$ polarization. As proof that the lowest-intensity peak in unpolarized reflectivity spectra belongs to the $\mathbf{E}\parallel\mathbf{c}$ polarization, we measured polarized photorefectance spectra in the energy range below 1.5 eV, which are shown in the inset of Fig. 7(a). These spectra clearly demonstrate that the reflectivity maximum at the lowest energy in Fig. 7(a) originates from the $\mathbf{E}\parallel\mathbf{c}$ polarization. The peak position of this transition is found at 1.43 eV using a photorefectance fitting line-shape procedure based on the third derivative of the primary spectra.⁴⁰ Thus, we conclude that *the lowest-energy gap in SrCuO_2 is at about 1.42 eV for the polarization along the Cu-O chains.*

Figure 8 represents the absorption spectra of SrCuO_2 measured at room temperature and 5 K for the incident light polarized along the \mathbf{c} and the \mathbf{a} axis. These spectra were calculated using the relation $\alpha(\omega) = (1/d) \ln\{[1 - R(\omega)]^2 / T(\omega)\}$, where R and T represent the reflectivity and transmission coefficient, while d is the thickness of the sample. As it can be seen from Fig. 8, there is a strong anisotropy in the positions of the absorption edges for these polarizations.

V. DISCUSSION

The experimental results given in Figs. 6–8 can be summarized as follows.

(i) A strong anisotropy of optical properties is clearly seen. In the direction perpendicular to the Cu-O chains ($\mathbf{E}\parallel\mathbf{a}$) the spectral weight is centered at about 1.8 eV. All other transitions at higher energies have smaller contributions to the dielectric function for this polarization. In the case of the $\mathbf{E}\parallel\mathbf{c}$ polarization [Fig. 6(b)] the spectra show very low intensity and the spectral weight for this polarization is shifted to higher energies at about 3.2 and 5.2 eV.

(ii) The lowest-energy gap appears at about 1.42 eV, well below the charge-transfer gap (1.7–2.0 eV) of other CuO-based materials.

(iii) The lowest-energy gap for $\mathbf{E}\parallel\mathbf{c}$ shows a very small energy change as the temperature is lowered, whereas the absorption edge of the corresponding gap for the $\mathbf{E}\parallel\mathbf{a}$ shifts to higher energies.

(iv) The higher-energy electron transitions appear at about 4.1 and 5.2 eV for both polarizations.

These features can be successfully explained in the framework of the electronic structure calculations, Sec. III B. The parameters of our model for correlated electrons, t , t_{yz} , and U , were fitted to the experimental value of the indirect Δ_0 gap ($\Delta_0 = 1.42$ eV) and an exchange energy along the chain (leg) $J = 0.18$ eV.⁵ We used also the ratio of exchange energies $J'/J = 0.16$ (J' represents the exchange energy between legs), because this value is in the middle of the range $J'/J = 0.1$ – 0.2 proposed for this kind of copper oxides.⁴¹ Using the relation between exchange and hopping energies $J = 4t^2/U$ and Eq. (5) for the lowest-energy gap, we estimated the other model parameters, $t = 0.30$ eV, $t_{yz} = 0.12$ eV, $U = 2.0$ eV. The obtained magnitude of the Anderson-Hubbard parameter of SrCuO_2 is somewhat lower than that ($U = 2.1$ eV) obtained previously by us in the electronic structure study of $\text{Sr}_{14}\text{Cu}_{24}\text{O}_{41}$.³⁶ The hopping energy $t = 0.3$ eV along the legs is larger than that in the case of $\text{Sr}_{14}\text{Cu}_{24}\text{O}_{41}$ ($t = 0.26$ eV) due to the difference between the exchange coupling constants: $J = 180$ meV in SrCuO_2 is larger than the $J = 128$ meV value in $\text{Sr}_{14}\text{Cu}_{24}\text{O}_{41}$. The coincidence of the Anderson-Hubbard parameters U for SrCuO_2 and $\text{Sr}_{14}\text{Cu}_{24}\text{O}_{41}$ is natural to expect because the local environment of Cu^{2+} ions is similar in these oxides and the on-site Coulomb repulsion is governed mainly by the electron interactions on the same copper d orbital.

The energy versus wave number curves for correlated electrons [Fig. 5(a)] show a large dispersion along the k_z direction (parallel to the Cu-O chains, along the \mathbf{c} axis) and no dispersion along the k_y direction, in agreement with the

LSDA calculations (Fig. 2). Nevertheless, the lowest-energy gap at about 1.42 eV appears for the transition from the Z to the Γ point of the BZ [indirect transition, denoted as Δ_0 in Fig. 5(a)]. The direct transition gaps Δ_2 , Δ_3 , and Δ_4 at the Γ (X) point of the BZ are found to be 1.88, 2.05, and 2.19 eV, respectively [see Fig. 5(b)].

According to our calculations in Sec. III B, the correlation gap Δ_0 , Eq. (5), represents the lowest-energy transitions between the split $3d_{y^2-z^2}$ - $3d_{y^2-z^2}$ states within each Cu atom. Thus, it is natural to expect a negligible temperature dependence of the correlation gap. In fact, experimental data presented in Fig. 8 show no temperature shift of the absorption edge for the $\mathbf{E}\parallel\mathbf{c}$ polarization. It means that SrCuO_2 belongs to the group of low-dimensional insulators with a correlation gap. Further support for this assumption can be found in the case of Sr_2CuO_3 , also a 1D cuprate. Maiti *et al.*⁴² assigned the gap, observed at about 1.5 eV in Sr_2CuO_3 , as an insulating gap of the correlated nature. Nevertheless, our Raman spectroscopy study⁹ clearly demonstrated that the resonance behavior in SrCuO_2 differs strongly from that in the 2D cuprates. Namely, the resonant Raman scattering shows that the infrared-active modes and their overtones resonate much more strongly for the laser energies near the charge-transfer gap in the 2D insulating cuprates.⁸ In 1D SrCuO_2 the infrared modes resonate at energies noticeably higher than the correlation gap Δ_0 .⁹ Finally, we have found that a spectral weight distribution similar to that given in Fig. 6(b) is also reported for Li_2CuO_2 for the light polarized along the chains.⁴³ This supports once again our findings that the electronic structure of the 1D cuprates differs significantly from that of the 2D cuprates.

In the inset of the Fig. 5(a) we show the Δ_0 gap dependence on the U parameter, Eq. (5), for the two different values of the interchain hopping t_{yz} at $t=0.30$ eV. The limiting case $t_{yz}=0$ represents one leg of the ladder or a single-chain structure that exists in Sr_2CuO_3 . As it is seen in the inset of Fig. 5(a), the interchain hopping reduces a gap. It means that the corresponding gaps in the single-chain compound Sr_2CuO_3 should be somewhat larger than that in SrCuO_2 . This agrees well with our experimental findings. Namely, the absorption edge in Sr_2CuO_3 is at 1.5 eV,⁴² about 5% higher than that in SrCuO_2 ; see Fig. 8.

The electron structure calculations for correlated electrons (Fig. 5) make it possible to compare to experimental data, not only the lowest-energy gap value. The peaks at 1.77 and 2 eV of the $\mathbf{E}\parallel\mathbf{a}$ $\varepsilon_2(\omega)$ spectra correspond to the L_{2-} - L_{1+} and L_{2-} - L_{2+} transitions at Γ and X points (Δ_2 and Δ_3 gaps), respectively. In the $\mathbf{E}\parallel\mathbf{c}$ polarized $\varepsilon_2(\omega)$ spectra we observed three very-low-intensity peaks at about 2.2, 2.6, and 3 eV. These transitions can be assigned as L_{1-} - L_{1+} (Δ_4), L_{2-} - L_{3+} , and L_{1-} - L_{3+} , respectively. Because of the very low intensity of these modes, it was hardly possible to extract their exact positions from the noise level. The energies of all possible electron transitions between occupied and empty states are shown in the inset of Fig. 5(b).

Now we discuss the two higher-energy features at about 4.1 and 5.2 eV. They have been already observed in many cuprates, as discussed in Ref. 44. Alonso *et al.*⁴⁴ have shown that in $\text{Nd}_{2-x}\text{Ce}_x\text{CuO}_4$ the transition at about 4 eV originates

from the $\text{Cu } 3d$ - $\text{Cu } 4p$ intraionic transition and the highest-energy transition about 5.2 eV occurs due to transition between the $\text{O } 2p$ and the $\text{Cu } 4s$ states. The existing band-structure calculations of SrCuO_2 are not detailed enough to corroborate this assignment.

Let us now consider Fig. 8, where the absorption coefficient spectra are presented. There is a large difference between the absorption-edge positions for the $\mathbf{E}\parallel\mathbf{c}$ and the $\mathbf{E}\parallel\mathbf{a}$ polarizations. Besides that, the slope of the absorption coefficient is higher for the $\mathbf{E}\parallel\mathbf{c}$ than the $\mathbf{E}\parallel\mathbf{a}$ polarization as a consequence of a quasi-1D character of this transition. A general approach to analyze the fundamental absorption edge is based on the use of the power-law behavior of $\alpha(\omega)$ in the vicinity of the band gap, E_{gap} . The absorption coefficient can be described as $\alpha(\omega)=A(\omega-E_{\text{gap}})^k$, where A is a slowly varying function that is regarded as a constant over the narrow range under study, and a number k depends on the nature of an electron transition from the occupied to the empty band. The k value is $\frac{1}{2}$ for a direct transition and 2 for an indirect one. Thus, the $\sqrt{\alpha(\omega)}\sim(\omega-E_{\text{gap}})$ dependence can be used to obtain the indirect-gap value by extrapolating the linear portion of this curve to intersect with the ω axis. The direct-gap position can be extracted from a maximum of the first derivative of $\alpha(\omega)$ [$\alpha'(\omega)\sim 1/\sqrt{\omega-E_{\text{gap}}}$]. This procedure is valid for a three-dimensional case and for the parabolic electron energy dispersions.

The absorption spectra for strongly correlated electron systems were analyzed using the density of states versus energy dependence of 1D (Ref. 45) or 3D (Ref. 46) semiconductors with parabolic energy dispersions. Actually, the dispersion branches in strongly correlated systems are parabolic in the vicinity of the high-symmetry points of the BZ. $\cos p=1-p^2/2$ around Γ (≈ 0) and $\cos p=-1+p^2/2$ around Z ($\approx \pi$). Furthermore, from the extrapolation of the linear part of the $\alpha(\omega)$ to the energy axis, we obtain the value of 1.52 eV (1.65 eV) for $\mathbf{E}\parallel\mathbf{c}$ ($\mathbf{E}\parallel\mathbf{a}$) polarization. This energy is higher (lower) than that obtained by ellipsometric or reflectivity measurements. Complete agreement with ellipsometric and reflectivity data is achieved when we consider *the $\mathbf{E}\parallel\mathbf{c}$ absorption edge as an indirect transition and the $\mathbf{E}\parallel\mathbf{a}$ absorption edge as a direct transition*, which is illustrated in the left and the right insets of Fig. 8. Thus, we have concluded that *the correlation gap in SrCuO_2 represents the indirect transition of carriers between the occupied and the empty correlated subbands*. The indirect transition requires a change in both energy and momentum of carriers as our band-structure calculations predict; see Fig. 5(a). It is well known that in semiconductors an electron momentum is conserved via an interaction with phonons.²⁶ For such a conclusion here, further experiments are necessary to clarify this point. They can be done by the transmission measurements through the samples of different thickness and/or comparison of photoluminescence with photorefectance spectra.

Quite recently, based on the Bethe ansatz solution for the Hubbard chain it was shown⁴⁷ that in an insulating state the optical conductivity can be described as $\sigma(\omega)\sim C(\omega-E_{\text{MH}})^{1/2}$, where E_{MH} is the (Mott-Hubbard) gap. Since

$\alpha(\omega) \sim \sigma(\omega)$, this dependence has the same power law as that we used for the direct electron transition.

For the $E_{||}$ polarization, the absorption edge shifts to higher energies by about 0.06 eV, when the temperature decreases from a room temperature to 5 K. For this electronic transition we cannot neglect hybridization of the Cu $3d$ with the O $2p$ bands. Thus, the absorption edge shifts to higher energies according to the change of the Cu-O distance with temperature. Besides that, this energy gap represents the transition between the dispersionless branches with very high effective electron masses and, consequently, with a strong influence of ligands. Because of that we believe that for the $E_{||}$ polarization the absorption-edge shift appears mainly due to dilatation of lattice by lowering the temperature.

In conclusion, we have investigated the electronic structure of the zigzag-chain compound SrCuO₂ combining polarized optical absorption, reflection, photorefectance, and pseudo-dielectric-function measurements with theoretical estimations. At 300 K these measurements yield the energy gaps 1.42 and 1.77 eV along and perpendicular to the Cu-O chains, respectively. The electronic structure of this oxide is

calculated using the LSDA with gradient corrections and the tight-binding method for the correlated electrons. The indirect (direct) gap value of 1.42 eV (1.86 eV) is found for the electron hopping energies between copper sites along legs, $t=0.30$ eV, and between them, $t_{yz}=0.12$ eV, with the Anderson-Hubbard parameter $U=2.0$ eV. The obtained experimental results and electronic structure calculations have shown that the SrCuO₂ zigzag-chain compound belongs to the low-dimensional insulators with a band gap of correlated nature.

ACKNOWLEDGMENTS

Z.V.P., V.A.I., and O.P.K. acknowledge support from the Research Council of the K.U. Leuven and DWTC. The work at the K.U. Leuven was supported by the Belgian IUAP and Flemish FWO and GOA Programs. M.J.K. and Z.V.P. thank Roman Herzog AvH, Bonn and University of Valencia, respectively, for partial financial support. V.A.I. acknowledges Yu. M. Kagan for fruitful discussions.

*Permanent address: Institute of Physics, 11080 Belgrade, P. O. Box 68, Yugoslavia.

[†]Present address: Department Natuurkunde, Universiteit Antwerpen, Universiteitsplein 1, B-2610 Belgium. On leave from N. S. Kurnakov Institute of the General and Inorganic Chemistry of the Russian Academy of Sciences, Leninskii prospect 31, 117907 Moscow.

¹Z. Hiroi, M. Takano, M. Azuma, Y. Takeda, and Y. Bando, *Physica C* **185-189**, 523 (1991).

²C. Kim, A. Y. Matura, Z. X. Shen, N. Motoyama, H. Eisaki, S. Uchida, T. Tohyama, and S. Maekawa, *Phys. Rev. Lett.* **77**, 4054 (1996).

³C. Kim, Z. X. Shen, N. Motoyama, H. Eisaki, S. Uchida, T. Tohyama, and S. Maekawa, *Phys. Rev. B* **56**, 15 589 (1997).

⁴N. Motoyama, H. Eisaki, S. Uchida, *Phys. Rev. Lett.* **76**, 3212 (1996).

⁵M. Matsuda, K. Katsumata, K. M. Kojima, M. Larkin, G. M. Luke, J. Merrin, B. Nachumi, Y. J. Uemura, H. Eisaki, N. Motoyama, S. Uchida, and G. Shirane, *Phys. Rev. B* **55**, R11 953 (1997).

⁶O. V. Misochko, S. Tajima, C. Urano, H. Eisaki, and S. Uchida, *Phys. Rev. B* **53**, R14 733 (1996).

⁷M. V. Abrashev, A. P. Litvinchuk, C. Thomsen, and V. N. Popov, *Phys. Rev. B* **55**, 9136 (1997).

⁸M. V. Abrashev, A. P. Litvinchuk, C. Thomsen, and V. N. Popov, *Phys. Rev. B* **55**, R8638 (1997).

⁹Z. V. Popović, M. J. Konstantinović, R. Gajić, C. Thomsen, U. Kuhlman, and A. Vietkin, *Physica C* (to be published); cond-mat/0010221 (unpublished).

¹⁰N. Nagasako, T. Oguchi, H. Fujisawa, O. Akaki, T. Yokoya, T. Takahashi, M. Tanaka, M. Hasegawa, and H. Takei, *J. Phys. Soc.* **66**, 1756 (1997).

¹¹Z. S. Popović and F. R. Vukajlović, *Solid State Commun.* **106**, 415 (1998).

¹²H. Wu, Q. Zheng, X. Gong, and H. Q. Lin, *J. Phys.: Condens. Matter* **11**, 4637 (1999); **12**, 5813 (2000).

¹³Chr. L. Taske and Hk. Müller-Buschbaum, *Z. Anorg. Allg. Chem.* **377**, 144 (1970).

¹⁴Y. Matsushita, Y. Oyama, M. Hasegawa, and H. Takei, *J. Solid State Chem.* **114**, 289 (1994).

¹⁵I. A. Zaliznyak, C. Broholm, M. Kibune, M. Nohara, and H. Takagi, *Phys. Rev. Lett.* **83**, 5370 (1999).

¹⁶H. Rosner, M. Divis, K. Koepnik, S. L. Drechsler, and H. Eschrig, *J. Phys.: Condens. Matter* **12**, 5809 (2000).

¹⁷<http://www.tuwien.ac.at/theochem/WIEN97/>; B. Blaha, K. Schwarty, and J. Luity, *Comput. Phys. Commun.* **59**, 399 (1990).

¹⁸J. P. Perdew, K. Burke, and M. Ernzerhof, *Phys. Rev. Lett.* **77**, 3865 (1996); **80**, 891 (1998).

¹⁹J. P. Perdew, J. A. Chevary, S. H. Vosko, K. A. Jackson, M. R. Pederson, D. J. Singh, and C. Fiolhais, *Phys. Rev. B* **46**, 6671 (1992).

²⁰P. Dufek, P. Blaha, V. Sliwko, and K. Schwartz, *Phys. Rev. B* **49**, 10 170 (1994).

²¹M. Knupfer, R. Neudert, M. Kielwein, S. Haffner, M. S. Golden, J. Fink, C. Kim, Z. X. Shen, M. Merz, N. Nücker, S. Schuppler, N. Motoyama, H. Eisaki, S. Uchida, Z. Hu, M. Domke, and G. Kaindl, *Phys. Rev. B* **55**, R7291 (1997).

²²P. Fulde, *Electron Correlations in Molecules and Solids*, 3rd ed. (Springer, Berlin, 1995), p. 189.

²³O. Gunnarsson and B. I. Lundqvist, *Phys. Rev. B* **13**, 4274 (1976).

²⁴J. P. Perdew and A. Zunger, *Phys. Rev. B* **23**, 5048 (1981).

²⁵N. E. Zein, *J. Phys. C* **17**, 2107 (1984).

²⁶P. Y. Yu and M. Cardona, *Fundamentals of Semiconductors* (Springer, Berlin, 1996).

²⁷M. S. Hybertsen and S. G. Louie, *Phys. Rev. B* **34**, 5390 (1986).

²⁸V. I. Anisimov, F. Aryasetiawan, and A. I. Lichtenstein, *J. Phys.: Condens. Matter* **9**, 767 (1997).

²⁹S. L. Dudarev, G. A. Botton, S. Y. Savrastov, C. J. Humphreys, and A. P. Sutton, *Phys. Rev. B* **57**, 1505 (1998).

³⁰V. I. Anisimov, J. Zaanen, and O. K. Andersen, *Phys. Rev. B* **44**,

- 943 (1991); P. Wei, Z. Q. Qi, *ibid.* **49**, 10 864 (1994).
- ³¹C. G. Olson, R. Liu, D. W. Lynch, R. S. List, A. J. Arko, B. W. Veal, Y. C. Chang, P. Z. Jiang, and A. P. Paulikas, *Phys. Rev. B* **42**, 381 (1990).
- ³²R. Manske, T. Buslaps, R. Claessen, M. Skibowski, and J. Fink, *Physica C* **162-164**, 1381 (1989).
- ³³J. Merino and R. H. McKenzie, *Phys. Rev. B* **62**, 2416 (2000).
- ³⁴N. N. Bogoljubov, *Selected Papers*, Vol. 2 (Naukova Dumka, Kiev, 1970, in Russian), p. 287.
- ³⁵V. A. Ivanov, Z. V. Popović, O. P. Khuong, and V. V. Moshchalkov, cond-mat/9909046 (unpublished).
- ³⁶Z. V. Popović, M. J. Konstantinović, V. A. Ivanov, O. P. Khuong, R. Gajić, A. Vietkin, and V. V. Moshchalkov, *Phys. Rev. B* **62**, 4963 (2000).
- ³⁷V. A. Ivanov, *J. Phys.: Condens. Matter* **6**, 2065 (1994); in *Studies of High- T_c Superconductors*, edited by A. Narlikar (Nova Science, New York, 1993), Vol. 11, pp. 331–352; *Physica C* **271**, 127 (1996); *Philos. Mag. B* **76**, 697 (1997).
- ³⁸K. Tsutsui, T. Tohyama, and S. Maekawa, *Phys. Rev. B* **61**, 7180 (2000).
- ³⁹V. A. Ivanov, K. Yakushi, and E. Ugolkova, *Physica C* **275**, 26 (1997).
- ⁴⁰D. E. Aspnes, in *Optical Properties of Solids*, edited by T. S. Moss, Vol. 2 of *Handbook on Semiconductors* (North-Holland, Amsterdam, 1980), p. 109; also Ref. 26, p. 317.
- ⁴¹T. M. Rice, S. Gopalan, and M. Sigrist, *Europhys. Lett.* **23**, 445 (1993).
- ⁴²K. Maiti, D. D. Sarma, T. Mizokawa, and A. Fujimori, *Phys. Rev. B* **57**, 1572 (1998).
- ⁴³Y. Mizuno, T. Tohyama, S. Maekawa, T. Osafune, N. Motoyama, H. Eisaki, and S. Uchida, *Phys. Rev. B* **57**, 5326 (1998).
- ⁴⁴M. I. Alonso, M. Garriga, S. Piñol, and M. Brinkmann, *Physica C* **299**, 41 (1998).
- ⁴⁵M. Dressel, A. Schwartz, G. Grüner, and L. Degiorgi, *Phys. Rev. Lett.* **77**, 398 (1996).
- ⁴⁶A. Zibold, H. L. Liu, S. W. Moore, J. M. Graybeal, and D. B. Tanner, *Phys. Rev. B* **53**, 11 734 (1996).
- ⁴⁷J. M. P. Carmelo, N. M. R. Peres, and P. D. Sacramento, *Phys. Rev. Lett.* **84**, 4673 (2000).